SCIENTIFIC REPORTS

OPEN

SUBJECT AREAS:
MOLECULAR DYNAMICS
PROTEIN FUNCTION PREDICTIONS

Received
29 November 2013

Accepted
12 March 2014

Published
8 April 2014

Correspondence and requests for materials should be addressed to M.N. (mnagaoka@is.nagoya-u.ac.jp)

Non-site-specific allosteric effect of oxygen on human hemoglobin under high oxygen partial pressure

Masayoshi Takayanagi[1,2,3], Ikuo Kurisaki[2] & Masataka Nagaoka[2,3]

[1]Venture Business Laboratory, Nagoya University, Furo-cho, Chikusa-ku, Nagoya 464-8601, Japan, [2]Graduate School of Information Science, Nagoya University, Furo-cho, Chikusa-ku, Nagoya 464-8601, Japan, [3]Core Research for Evolutional Science and Technology, Japan Science and Technology Agency, Honmachi, Kawaguchi 332-0012, Japan.

Protein allostery is essential for vital activities. Allosteric regulation of human hemoglobin (HbA) with two quaternary states T and R has been a paradigm of allosteric structural regulation of proteins. It is widely accepted that oxygen molecules (O_2) act as a "site-specific" homotropic effector, or the successive O_2 binding to the heme brings about the quaternary regulation. However, here we show that the site-specific allosteric effect is not necessarily only a unique mechanism of O_2 allostery. Our simulation results revealed that the solution environment of high O_2 partial pressure enhances the quaternary change from T to R without binding to the heme, suggesting an additional "non-site-specific" allosteric effect of O_2. The latter effect should play a complementary role in the quaternary change by affecting the intersubunit contacts. This analysis must become a milestone in comprehensive understanding of the allosteric regulation of HbA from the molecular point of view.

Complex processes of signaling in the living cell are comprised of many allosteric interactions between proteins[1]. Thus controlling the allostery is emerging as a promising approach for pharmaceutical drug discovery and allosteric ligands for G protein-coupled receptors have been approved as medicines[2]. Allosteric regulation is assumed to be triggered by site-specific ligand binding to allosteric sites, which are distinct from the orthosteric ligand binding site. As a paradigm of such allosteric regulation, allostery of human hemoglobin (HbA), which is an oxygen transport protein composed of two α and two β subunits, has long been thoroughly studied[3–5]. Under the circumstances, it is widely accepted that O_2 acts as a "site-specific" homotropic allosteric effector, or the successive O_2 binding to the four subunit hemes triggers quaternary change from the low O_2 affinity T state to the high affinity R one. The MWC model[6] is one of the most successful models to explain the sigmoidal oxygen binding curve on the basis of the homotropic allosteric mechanism. From the molecular point of view, the homotropic allostery was additionally explained by including the interaction energies of intersubunit contacts which stabilize the T state structure[7]; when O_2 binds to the heme, the tertiary structural change of the HbA subunit is triggered by the heme deformation from the domed structure to the planar one and, as a result, those contacts are destabilized to drive the T to R transition[3]. In fact, in HbA subunit analogous protein, myoglobin (Mb), it has been elucidated that the heme deformation by the ligand (O_2 or CO) binding or dissociation triggers structural relaxation in the whole protein[8–13]. However, our current molecular dynamics (MD) simulation revealed that, even without site-specific O_2 binding to the heme, the solution environment of high O_2 partial pressure enhances the quaternary structural change from T to R, suggesting the "non-site-specific" allosteric effect of O_2.

Using the statistical ensemble MD approach[11–14], we executed 128 independent 8 nanosecond (ns) MD simulations starting from the T state deoxy-HbA crystal structure[15] at the physiological condition (310 K and 1 atm) in both aqueous solvent (MD^{wat} with ~12000 H_2O molecules) and oxygen-rich aqueous solvent with $[O_2]$ = 0.55 mol/L (MD^{O2} with 120 O_2 and ~12000 H_2O molecules), which is about 500 times higher than that in the O_2 saturation concentration at ambient conditions, ~1 mmol/L. This high partial pressure was applied to amplify the non-site-specific effect of O_2. We artificially ignored the O_2 binding to the heme and thus all the hemes were retained in the domed structure for the purpose to exclude the heme O_2 binding effect.

Results

Global evidence of quaternary change: transition in intersubunit dihedral angle and RMSD. It was reported that spontaneous T to R quaternary transition reproducibly occurred in the submicrosecond MD simulations of

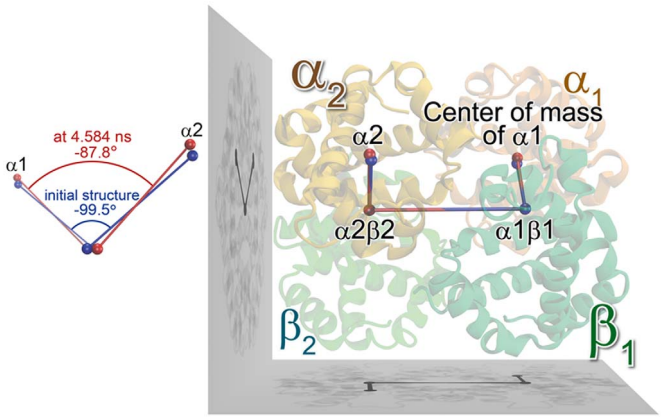

Figure 1 | T state crystal (initial MD) structure of HbA (PDB ID: 2DN2). The dihedral angle χ defined by the four centers of mass, i.e., those of α_1 subunit, $\alpha_1\beta_1$ dimer, $\alpha_2\beta_2$ dimer, and α_2 subunit, is shown as ball and stick drawing. The blue color drawing is the COMs of the initial T state structure with $\chi = -99.5$ degrees. The red one is those from a typical T to R quaternary change trajectory at 4.584 ns with $\chi = -87.8$ degrees.

HbA starting from the T state structure[16,17]. Our simulations also exhibited the T to R quaternary changes. Because the quaternary change is accompanied with $\alpha_1\beta_1$ ($\alpha_2\beta_2$) dimer rotation[3,18], the temporal change of the intersubunit dihedral angle χ, defined by the four centers of mass (COMs) of subunits (see Fig. 1), is an index of the quaternary change; −99.5 and −89.0 degrees for T and R crystal structures (PDB ID: 2DN2 and 2DN1[15]), respectively. Figs. 2 gives one of the typical trajectories of MD^{O2} in which the T to R quaternary change occurred. Until 3 ns, the HbA structure kept its initial T structure, and later, χ changed during $t = 3.0$ to 4.5 ns and reached −87 degrees, strongly correlating with the decrease of $RMSD^R$ to 1.4 Å (Fig. 2a).

Local evidence of quaternary change: switch region rearrangement. Furthermore, local structural changes in the $\alpha_1\beta_2$ ($\alpha_2\beta_1$) switch region were also consistent with the T to R change: β_2His97 moves from the groove between α_1Pro44 and α_1Thr41 to that between α_1Thr38 and α_1Thr41[4,18]. This rearrangement also occurred in this trajectory during $t = 3$ to 4.25 ns (Fig. 2b). The α_1Thr38-β_2His97 distance decreased from 11 to 5 Å and that of α_1Pro44-β_2His97 conversely increased from 5 to 11 Å (Fig. 2c). Other trajectories of MD^{O2} and MD^{WAT} in which the quaternary change occurred also revealed the similar behaviors of the χ, $RMSD^R$, and switch region structural changes (Supplementary Figs. S1 and S2).

Other regions also revealed T to R quaternay change characteristics. Breakages of intersubunit salt bridges α_1Lys40-β_2His146 and α_1Tyr42-β_2Asp99 occur by the T to R quaternary change[15]. These breakages were also observed in the quaternary change trajectory (Supplementary Fig. S3). Meanwhile, in the $\alpha_1\beta_2$ ($\alpha_2\beta_1$) hinge region (also denoted as flexible joint region), the intersubunit contacts were retained and there were no significant structural rearrangements during the quaternary change (Supplementary Fig. S4) as crystallographically observed[19].

Non-site-specific allostery emerged in the intersubunit dihedral angle distribution. To investigate the effect of high O_2 partial pressure, statistical comparison between the 128 MD trajectories of MD^{O2} and MD^{wat} was carried out. When the time average of χ over 7–8 ns is larger than −95 degrees, the trajectory is defined as a *quaternary change trajectory*. On this definition, the number of quaternary change trajectories were 10 and 4 for MD^{O2} and MD^{wat}, respectively, suggesting that the high O_2 partial pressure enhances the T to R quaternary change.

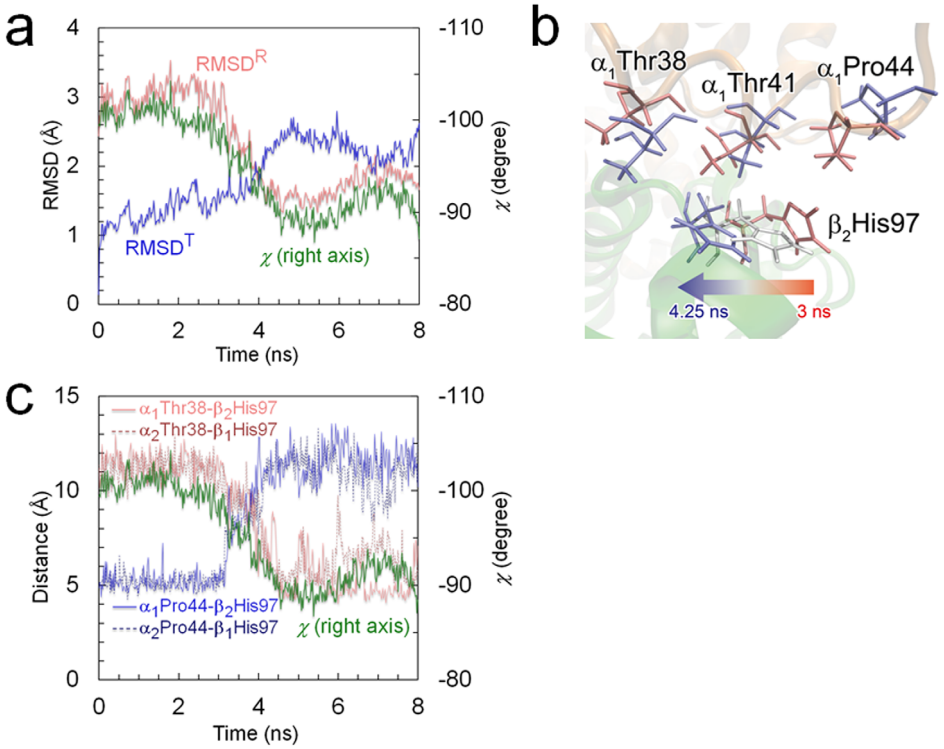

Figure 2 | T to R quaternary structural change. A typical quaternary change trajectory of MD^{O2}. (a) Changes of the RMSD to the T ($RMSD^T$) and R ($RMSD^R$) crystal structures and the intersubunit dihedral angle χ. (b) Structural rearrangement at the switch region of the $\alpha_1\beta_2$ interface. Important residues are drawn at 3 ns (red) and 4.25 ns (blue) with the intermediate structure of β_2His97 at 3.7 ns (white). (c) Distance changes between the COM of the βHis97 sidechain and the COMs of αThe38 and αPro44 at the two switch regions plotted with χ.

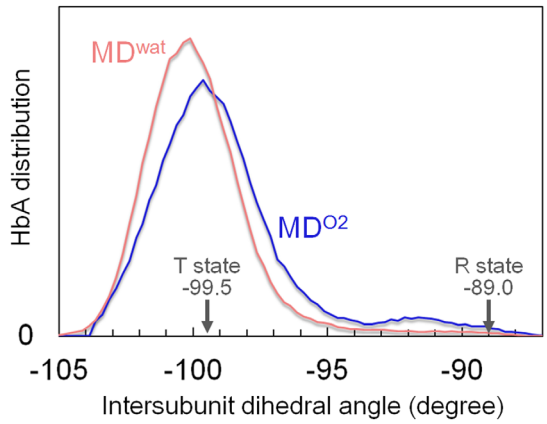

Figure 3 | χ Distribution shift by high O_2 partial pressure. Distributions of the intersubunit dihedral angle χ calculated from 128 independent MD trajectories during 7–8 ns. The dihedral angles were sampled every 1 ps from 7 to 8 ns of each trajectory (in total 128,000 samples from 128 trajectories).

To obtain further structural insight, we investigated the χ distributions of MD^{O2} and MD^{wat} during 7–8 ns (Fig. 3). The two distribution curves were well fitted by the sum of three Gaussian functions as

$$f(\chi)=\sum_{i=1}^{3} g_i(\chi)=\sum_{i=1}^{3} A_i \frac{1}{\sqrt{2\pi\delta\chi_i^2}}\exp\left\{-\frac{(\chi-\chi_i^{M})^2}{2\delta\chi_i^2}\right\}. \quad (1)$$

The fitted parameters (A_i, $\delta\chi_i$, χ^{M}_i) and the fitted curves are summarized in the Supplementary Table S1 and Fig. S5. For MD^{wat}, the main distribution $g_1(\chi)$ with the mean angle (χ_1^{M}) and width ($\delta\chi_1$) of −100.2 and 1.54 degrees was obtained. Meanwhile, for MD^{O2}, the main distribution was −99.6 degrees mean angle and 1.75 degrees width.

The comparison of MD^{O2} and MD^{wat} distributions allows us to conclude that the solution environment of high O_2 partial pressure enhances the T to R quaternary change from the following two aspects. First, from the 0.6 degrees peak position shift of the main distribution toward the R state (from −100.2 (MD^{wat}) to −99.6 (MD^{O2}) degrees), the T state structure is biased toward the R state. Second, from the width increase from 1.54 (MD^{wat}) to 1.75 (MD^{O2}) degrees, the global structural fluctuation of the T state, which would contribute to the T to R quaternary change, is enhanced. The observed enhancement can be considered as the "non-site-specific" allosteric effect, or another allosteric regulation by O_2 without binding to the heme.

Discussion

Our ensemble MD simulation revealed that, even without the heme deformation by the O_2 binding to the heme, the solution environment of high O_2 partial pressure itself enhances the quaternary structural change from T to R. This means that the traditional site-specific allosteric regulation by O_2 binding to the heme is not necessarily the only one unique mechanism of O_2 allostery and the additional non-site-specific regulation does exist. From a molecular point of view, we propose following two hypothetical mechanisms of the non-site-specific allostery of O_2.

First is the internal effect: O_2 molecules enter the hydrophobic cavities inside HbA subunits[20] and trigger the tertiary structural changes to enhance the T to R quaternary change. In MD^{O2} simulations, hydrophobic O_2 molecules tended to escape from water and prefer the hydrophobic environment on the surface or inside HbA subunits[14]. The O_2 migrations between inside cavities would bring about the tertiary structural changes of HbA subunits since it was

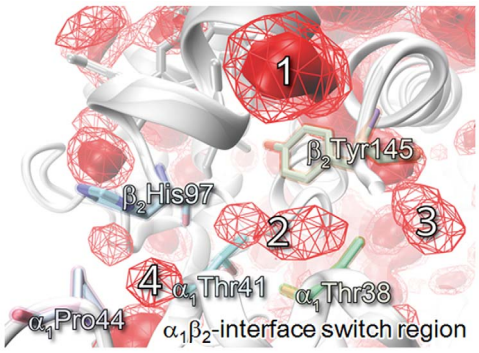

Figure 4 | Distribution of O_2 oxygen atoms around switch region. Distribution of O_2 oxygen atoms calculated from 128 MD trajectories during 7 to 8 ns in the vicinity of the switch region at the $\alpha_1\beta_2$-interface switch region. Locations with density >0.05 $Å^{-3}$ and >0.1 $Å^{-3}$ are drawn with red wire frame and solid surface, respectively. Since the average density in the bulk solvent region (distance to the nearest protein atom >4.0 Å) is about 0.005 $Å^{-3}$, the wire frame and solid surface regions are 10 and 20 times denser than that in the bulk solvent, respectively. Four high density locations around the switch region are numbered in descending order of the peak density.

observed that, in Mb, structural changes occur in response to the ligand migrations between cavities[21–23]. In particular, these reported structural changes in response to the CO transitions between the heme pocket and Xe4 cavity included displacements of the F helix, which forms the switch region of HbA β subunit[22] and hence would affect the stability of the T state structure.

Second is the surface effect: the existence of O_2 around the subunit interfaces weakens the contacts which stabilize the T state structure[3] by affecting the surface residues directly and/or indirectly through perturbing the behavior of water molecules. In fact, there are obviously high O_2 density locations in the vicinity of the switch region (Fig. 4). Thus it should be possible that the existance of O_2 directly affects the switch region residues through steric hinderance to weaken the contacts, while O_2 also influences surface water molecules to indirectly affect the switch region residues. In general, the characteristic constants of water molecules near the protein surfaces, such as diffusion constant[24], can be different from that in bulk solvent. Moreover, it has been reported that the number of interfacial water molecules changes during quaternary changes in hemoglobins[25–28], suggesting the important roles of the number of interfacial water molecules in the quaternary regulation. Thus, we can conjecture that the existence of O_2 would perturb the behavior of water molecules, e.g., as the deviation of diffusion constants and the number of interfacial water molecules around the surfaces, and, as a result, indirectly weaken the intersubunit contacts to enhance the T to R quaternary change.

The O_2 partial pressure applied in this work (0.55 mol/L) is about 500 times higher than that in the O_2 saturation concentration at ambient conditions (~1 mmol/L). We anticipate that the non-site-specific effects should be also observed under the ambient conditions for the following three reasons. First, our previous computational analysis with the same concentration 0.55 mol/L reproduced the rate constants of O_2 entry into the binding sites of HbA subunits[14]. Assuming a kinetic model of O_2 entry

$$Hb^x + O_2 \xrightarrow{k^x_{entry}} Hb^x : O_2, \quad (2)$$

where x denotes subunit ($x = \alpha$ or β) and $Hb^x : O_2$ is the situation of O_2 in the binding site, the rate of O_2 entry is $k^x_{entry}[O_2][Hb^x]$ and the rate constants k^{α}_{entry} and k^{β}_{entry} are calculated to be 45 and 99 $(\mu mol/L)^{-1}s^{-1}$, respectively. These values are consistent with

experimentally observed values after temperature correction, 48–69 and 81–131 $(\mu mol/L)^{-1}s^{-1}$ for α and β subunits, respectively. This consistency indicates that the concentration 0.55 mol/L is within the linearly extrapolatable range by the O_2 concentration, as the rate constants can be estimated by the formula $k^x_{entry}[O_2][Hb^x]$. Second, the "effective" O_2 concentration around HbA is higher than the bulk concentration. As discussed above, hydrophobic O_2 molecules prefer the hydrophobic environment near the HbA surface and there are several high O_2 density regions, whose density is an order of magnitude higher than that in the bulk solvent region (Fig. 4). Therefore, compared to the bulk concentration, the "effective" O_2 concentration around HbA is higher. This should partially narrow the concentration gap between the current simulation conditions and ambient conditions. Third, a preliminary ensemble MD simulation at one-tenth concentration, 0.055 mol/L (MD^{lowO2} with 12 O_2 and ~12000 H_2O molecules) also revealed the non-site-specific effect. We executed 40 MD simulations for 8 ns at the 0.055 mol/L concentration and calculated the χ distribution during 7–8 ns (Supplementary Fig. S6). The MD^{lowO2} distribution is apparently shifted toward the R state as in MD^{O2}.

From an experimental point of view, it is necessary to analyze the number of O_2 molecules around or inside HbA subunits because the number of O_2-bound heme in tetrameric HbA, which is the traditional index of O_2 allostery and is easily observed by spectroscopy, cannot capture the non-site-specific O_2 allosteric contributions. In particular, as Tomita et al. discussed in Mb case[29], accurate measurement of the heme:O_2 stoichiometry with modern instrumentation is desired to verify the traditionally employed stoichiometry 1 : 1, which assumes that only one O_2 binds to the heme and there is effectively no O_2 in the hydrophobic cavities or near the surfaces of HbA subunits. The stoichiometry greater than 1 : 1 is plausible by hydrophobic interactions between O_2 and HbA and means that HbA subunits can carry excess O_2 in their cavities and/or surfaces, or the "effective" O_2 concentration around HbA is higher than bulk concentarion, and support the existence of the non-site-specific effect.

The current non-site-specific effect should provide a complementary mechanism to account for the cleavages of intersubunit contacts during the T to R quaternary change of HbA in high O_2 concentration environment from the molecular point of view. With respect to the displacements in the heme average strucutre, the O_2-heme binding itself brings about very small structural rearrangements: a comparison of high resolution crystal structures of Mb revealed that the heme iron atom is 0.290 Å displaced by ligand binding[10]. Since the immediate displacements in the residues distant from the heme within 20 ps after ligand phosolysis are smaller than those neighboring to the heme because of the elastic behavior of Mb[11], the immediate displacements propagated to the residues composing the intersubunit contacts must be smaller than the iron displacement. It is not obvious how such a small immediate displacements could cleavage the contacts, although it was in fact experimentally obserbed that the T to R quaternary change occurs after microseconds of ligand dissociation[30]. Meanwhile, by the dynamic non-equilibrium MD approach in Mb, it was shown that a large structural fluctuation in the FG-corner (that of β subunit forms the switch region in HbA) was brought about by the ligand dissociation and recombination to the heme[31]. Together with this structural fluctuation effect, O_2 molecules located near the intersubunit contacts as in Fig. 4 can interact with the contacts, playing a complementary role in cleavage of the contacts.

The non-site-specific effect can also be an important factor in allosteric structural regulation in other proteins. For example, in muscarinic receptors, orthosteric ligands were observed to function as an allosteric modulator[32] or weakly bind to the allosteric sites[33], indicating that the ligands can interact with multiple sites; not only the orthosteric site but also allosteric sites. In particular, for allosteric proteins in which the distance between orthosteric and allosteric sites is so far-away that direct structural perturbation between the sites seems to be unlikely, the multiple interaction sites between proteins and ligands, most of which are invisible by the X-ray crystallography because of their small occupancy, can help the structural rearrangements at the orthosteric sites. The concept of non-site-specific allostery should facilitate further understanding of allosteric regulation process depending on the concentration of effectors from the atomistic point of view.

Methods

The MD simulation force field parameters were identical to our previous work[14]. All the MD simulations were executed by AMBER 9 pmemd module[34]. The initial HbA structure was retrieved from the T state deoxy-HbA crystal (PDB ID: 2DN2)[15] and immersed in the periodic boundary TIP3P water box with 12023 water molecules and two chloride counterions, yielding the MD^{wat} system. In addition, 120 water molecules were replaced by 120 O_2 molecules to prepare MD^{O2} system. We executed 128 independent MD simulations for MD^{wat} and MD^{O2} systems, respectively, according to the following procedure with different initial atomic velocities. First, we executed 300 ps high temperature NVT MD simulations at 700 K with the structure restraints on the protein. Second, equilibration NPT MD simulations for 200 ps at the target temperature 310 K and pressure 1 atm were executed with the protein restraint. Then production NPT MD simulations at 1 atm and 310 K were executed for 8 ns without any restraints. All the images of protein structures were drawn with VMD 1.9.1[35]. The density map in Fig. 4 was calculated by "VolMap Tool" in VMD with the parameters 1.0 Å resolution and 1.0 × radius atom size.

1. Nussinov, R., Tsai, C.-J. & Ma, B. The underappreciated role of allostery in the cellular network. *Annu. Rev. Biophys.* **42**, 169–189 (2013).
2. Wootten, D., Christopoulos, A. & Sexton, P. M. Emerging paradigms in GPCR allostery: implications for drug discovery. *Nat. Rev. Drug Discov.* **12**, 630–644 (2013).
3. Perutz, M. F., Wilkinson, A. J., Paoli, M. & Dodson, G. G. The stereochemical mechanism of the cooperative effects in hemoglobin revisited. *Annu. Rev. Biophys. Biomol. Struct.* **27**, 1–34 (1998).
4. Safo, M. K., Ahmed, M. H., Ghatge, M. S. & Boyiri, T. Hemoglobin-ligand binding: understanding Hb function and allostery on atomic level. *Biochim. Biophys. Acta* **1814**, 797–809 (2011).
5. Bellelli, A. Hemoglobin and cooperativity: Experiments and theories. *Curr. Protein Pept. Sci.* **11**, 2–36 (2010).
6. Monod, J., Wyman, J. & Changeux, J.-P. On the nature of allosteric transitions: A plausible model. *J. Mol. Biol.* **12**, 88–118 (1965).
7. Szabo, A. & Karplus, M. A mathematical model for structure-function relations in hemoglobin. *J. Mol. Biol.* **72**, 163–97 (1972).
8. Straub, J. E. & Karplus, M. Molecular dynamics study of the photodissociation of carbon monoxide from myoglobin: Ligand dynamics in the first 10 ps. *Chem. Phys.* **158**, 221–248 (1991).
9. Meller, J. & Elber, R. Computer simulations of carbon monoxide photodissociation in myoglobin: structural interpretation of the B states. *Biophys. J.* **74**, 789–802 (1998).
10. Kachalova, G. S., Popov, A. N. & Bartunik, H. D. A Steric Mechanism for Inhibition of CO Binding to Heme Proteins. *Science* **284**, 473–476 (1999).
11. Takayanagi, M., Okumura, H. & Nagaoka, M. Anisotropic structural relaxation and its correlation with the excess energy diffusion in the incipient process of photodissociated MbCO: high-resolution analysis via ensemble perturbation method. *J. Phys. Chem. B* **111**, 864–869 (2007).
12. Takayanagi, M., Iwahashi, C. & Nagaoka, M. Structural dynamics of clamshell rotation during the incipient relaxation process of photodissociated carbonmonoxy myoglobin: statistical analysis by the perturbation ensemble method. *J. Chem. Phys. B* **114**, 12340–12348 (2010).
13. Takayanagi, M. & Nagaoka, M. Incipient structural and vibrational relaxation process of photolyzed carbonmonoxy myoglobin: statistical analysis by perturbation ensemble molecular dynamics method. *Theor. Chem. Acc.* **130**, 1115–1129 (2011).
14. Takayanagi, M., Kurisaki, I. & Nagaoka, M. Oxygen Entry through Multiple Pathways in T-State Human Hemoglobin. *J. Phys. Chem. B* **117**, 6082–6091 (2013).
15. Park, S.-Y., Yokoyama, T., Shibayama, N., Shiro, Y. & Tame, J. R. H. 1.25 Å resolution crystal structures of human haemoglobin in the oxy, deoxy and carbonmonoxy forms. *J. Mol. Biol.* **360**, 690–701 (2006).
16. Hub, J. S., Kubitzki, M. B. & de Groot, B. L. Spontaneous quaternary and tertiary T-R transitions of human hemoglobin in molecular dynamics simulation. *PLoS comput. Biol.* **6**, e1000774 (2010).
17. Tekpinar, M. & Zheng, W. Coarse-grained and all-atom modeling of structural states and transitions in hemoglobin. *Proteins* **81**, 240–252 (2013).
18. Mouawad, L., Perahia, D., Robert, C. H. & Guilbert, C. New insights into the allosteric mechanism of human hemoglobin from molecular dynamics simulations. *Biophys. J.* **82**, 3224–3245 (2002).

19. Baldwin, J. & Chothia, C. Haemoglobin: the structural changes related to ligand binding and its allosteric mechanism. *J. Mol. Biol.* **129**, 175–220 (1979).
20. Savino, C. *et al.* Pattern of cavities in globins: the case of human hemoglobin. *Biopolymers* **91**, 1097–1107 (2009).
21. Schotte, F. *et al.* Watching a protein as it functions with 150-ps time-resolved x-ray crystallography. *Science* **300**, 1944–1947 (2003).
22. Nishihara, Y., Kato, S. & Hayashi, S. Protein collective motions coupled to ligand migration in myoglobin. *Biophys. J.* **98**, 1649–1657 (2010).
23. Tsuduki, T., Tomita, A., Koshihara, S., Adachi, S. & Yamato, T. Ligand migration in myoglobin: A combined study of computer simulation and x-ray crystallography. *J. Chem. Phys.* **136**, 165101 (2012).
24. Yu, I. & Nagaoka, M. Slowdown of water diffusion around protein in aqueous solution with ectoine. *Chem. Phys. Lett.* **388**, 316–321 (2004).
25. Knapp, J. E., Bonham, M. A., Gibson, Q. H., Nichols, J. C. & Royer, W. E. Residue F4 plays a key role in modulating oxygen affinity and cooperativity in Scapharca dimeric hemoglobin. *Biochemistry* **44**, 14419–14430 (2005).
26. Kim, K. H. *et al.* Direct Observation of Cooperative Protein Structural Dynamics of Homodimeric Hemoglobin from 100 ps to 10 ms with Pump-Probe X-ray Solution Scattering. *J. Am. Chem. Soc.* **134**, 7001–7008 (2012).
27. Gnanasekaran, R., Xu, Y. & Leitner, D. M. Dynamics of water clusters confined in proteins: a molecular dynamics simulation study of interfacial waters in a dimeric hemoglobin. *J. Phys. Chem. B* **114**, 16989–16996 (2010).
28. Colombo, M. F., Rau, D. C. & Parsegian, V. A. Protein solvation in allosteric regulation: a water effect on hemoglobin. *Science* **256**, 655–659 (1992).
29. Tomita, A., Kreutzer, U., Adachi, S., Koshihara, S. & Jue, T. 'It's hollow': the function of pores within myoglobin. *J. Exp. Biol.* **213**, 2748–2754 (2010).
30. Cammarata, M., Levantino, M., Wulff, M. & Cupane, A. Unveiling the timescale of the R-T transition in human hemoglobin. *J. Mol. Biol.* **400**, 951–962 (2010).
31. Cottone, G., Lattanzi, G., Ciccotti, G. & Elber, R. Multiphoton absorption of myoglobin-nitric oxide complex: relaxation by D-NEMD of a stationary state. *J. Phys. Chem. B* **116**, 3397–3410 (2012).
32. Redka, D. S., Pisterzi, L. F. & Wells, J. W. Binding of orthosteric ligands to the allosteric site of the M(2) muscarinic cholinergic receptor. *Mol. Pharmacol.* **74**, 834–843 (2008).
33. Kruse, A. C. *et al.* Structure and dynamics of the M3 muscarinic acetylcholine receptor. *Nature* **482**, 552–556 (2012).
34. Case, D. A. *et al.* The Amber biomolecular simulation programs. *J. Comput. Chem.* **26**, 1668–1688 (2005).
35. Humphrey, W., Dalke, A. & Schulten, K. VMD: visual molecular dynamics. *J. Mol. Graph.* **14**, 33–38 (1996).

Acknowledgments

This work was partially supported by a Grant-in-Aid for the 21st Century COE program "Frontiers of Computational Science" at Nagoya University and also by a Grant-in-Aid for Science Research from the Ministry of Education, Culture, Sport, Science and Technology in Japan and the Core Research for Evolutional Science and Technology (CREST) "Creation of Innovative Functional Materials with Advanced Properties by Hyper-nano-space Design" and "Establishment of Molecular Technology towards the Creation of New Functions" from the Japan Science and Technology Agency. I.K., also thanks for the support from Japan Society for the Promotion of Science (JSPS) by the Research Fellowship for Young Scientist.

Author contributions

M.N. conceived the project and M.T. designed the computational procedure. M.T. performed the calculations, prepared the figures and wrote a first draft of the manuscript. M.T., I.K. and M.N. discussed the results and wrote the manuscript. M.N. supervised all aspects of this work.

Additional information

Supplementary information accompanies this paper at http://www.nature.com/scientificreports

Competing financial interests: The authors declare no competing financial interests.

How to cite this article: Takayanagi, M., Kurisaki, I. & Nagaoka, M. Non-site-specific allosteric effect of oxygen on human hemoglobin under high oxygen partial pressure. *Sci. Rep.* **4**, 4601; DOI:10.1038/srep04601 (2014).